

On the Theory of Directional Solidification in the Presence of a Mushy Zone

D. V. Alexandrov^{a,*}, I. G. Nizovtseva^a, I. V. Alexandrova^a, A. A. Ivanov^a, I. O. Starodumov^a,
L. V. Toropova^a, O. V. Gusakova^b, and V. G. Shepelevich^c

^aUral Federal University named after the First President of Russia B.N. Yeltsin, Yekaterinburg, Russia

^bInternational Sakharov Environmental Institute of Belarusian State University, Minsk, Belarus

^cBelarusian State University, Minsk, Belarus

*e-mail: dmitri.alexandrov@urfu.ru

Received July 25, 2018; revised October 12, 2018; accepted January 11, 2019

Abstract—A model is developed for the directional solidification of a binary melt with a two-phase zone (mushy zone), where the fraction of the liquid phase is described by a space–time scaling relation. Self-similar variables are introduced and the interphase boundary growth is inversely proportional to the square root of time. The mathematical model of the process is reformulated using self-similar variables. Exact self-similar solutions of heat-and-mass transfer equations are determined in the presence of two mobile phase-transition boundaries, namely, solid–mushy zone and mushy zone–liquid ones. The temperature and impurity concentration distributions in the solid phase, the mushy zone, and the melt are found as integral expressions. A decrease in the dimensionless cooled-boundary temperature leads to an increase in the solidification rate and the fraction of the liquid phase. The solidification rate, the parabolic growth constants, and the fraction of the liquid phase at the solid–mushy zone boundary are determined depending on the scaling parameter and the thermophysical constants of the solidifying melt. The positions of the solid–mushy zone and mushy zone–binary melt phase transition boundaries are found. The dependences of the solidification rate (inversely proportional to the square root of time) are analyzed. The scaling parameter significantly is shown to substantially affect the solidification rate and the fraction of the liquid phase in the phase transformation region. The developed model and the method of its solution can be generalized to the case of directional solidification of multicomponent melts in the presence of several phase transformation regions (e.g., main and cotectic two-phase zones during the solidification of three-component melts).

Keywords: phase transitions, solidification, mushy zone

DOI: 10.1134/S0036029521020026

INTRODUCTION

A large number of solidification processes are described using the classical Stefan thermodiffusion model with a flat interface between a purely solid material and a liquid melt [1–5]. The mathematical model of the process includes heat conduction and diffusion equations for a dissolved impurity written in solid and liquid phases; initial conditions; and boundary conditions of heat–mass balance, temperature continuity, and the concentration jump at the solidification front. However, when a solid phase grows, a dissolved impurity is displaced into the surrounding melt. The impurity displacement intensity depends on the chemical composition of the dissolved impurities (from the melt undergoing phase transformation) and on the solidification rate in the case of high-speed solidification [6–9]. In time, the impurity concentration gradient (multiplied by the slope of the liquidus line) at the solidification front can exceed the tem-

perature gradient, which leads to the appearance of concentration supercooling [3, 10–13]. The appearance of a supercooled melt layer in front of the solidification front creates favorable conditions for the development of morphological instability, the growth of solid phase protrusions deep into the melt, and the nucleation and growth of solid phase elements [15–23]. In other words, a two-phase region, i.e., a mushy zone, forms before the solidification front [24–29]. The processes of solid phase growth in this zone determine the dynamic characteristics of the solidification process and the properties of the solidifying material. A large number of various realizations of the solid growth process in a supercooled two-phase region are known, and they are described by various mathematical models (see, e.g., [30–39]). In this work, we consider the theory of directional solidification where the liquid phase density in the mushy zone is described using the space–time scaling dependence [40].

HEAT-AND-MASS TRANSFER EQUATIONS

Consider the directional solidification of a binary melt along the spatial x axis (Fig. 1). The process area is divided into the following three regions: a solid phase, mushy zone, and a melt. Let $\Sigma(\tau)$ and $L(\tau)$ be the coordinates of the boundaries of the solid phase–mushy zone and mushy zone–melt regions, respectively. These boundaries move along the x axis due to given temperature conditions, which provide solidification. The diffusion of an impurity in the mushy zone ($\Sigma(\tau) < x < L(\tau)$) is described by the equation

$$S \frac{\partial}{\partial \tau} \int_x^{x+\Delta x} c_m(\xi, \tau) \rho(\xi, \tau) d\xi \quad (1)$$

$$= -[S_l(x+\Delta x, \tau) j(x+\Delta x, \tau) - S_l(x, \tau) j(x, \tau)],$$

where S and S_l are the total cross section of the sample and the cross section occupied by the liquid phase, respectively; c_m is the impurity concentration determined in the liquid phase; ρ is the volume fraction of the liquid phase in the mushy zone; and τ is the time.

Diffusion flux j is determined by classical Fick's law $j = -D_l \nabla c_m$, where D_l is the diffusion coefficient of the impurity. The relation between S and S_l is described using the simplest law $S_l = S p$. Substituting this relation into Eq. (1), using the mean-value theorem to transform the integral term, multiplying the equation by Δx^{-1} , and going to the limit $\Delta x \rightarrow 0$, we obtain

$$\frac{\partial}{\partial \tau} (c_m \rho) = D_l \frac{\partial}{\partial x} \left(\rho \frac{\partial c_m}{\partial x} \right), \quad \Sigma(\tau) < x < L(\tau). \quad (2)$$

The diffusion equation in the melt is written in the traditional form

$$\frac{\partial c}{\partial \tau} = D_l \frac{\partial^2 c}{\partial x^2}, \quad x > L(\tau), \quad (3)$$

where c_l is the impurity concentration in the liquid phase. The impurity diffusion in the solid phase is neglected.

The heat conduction equation in mushy zone is derived similarly to Eq. (2) and has the form

$$\left(C_l \rho + C_s \rho (1-p) \right) \frac{\partial \theta_m}{\partial \tau} = \frac{\partial}{\partial x} \left(\lambda \rho \frac{\partial \theta_m}{\partial x} \right), \quad \Sigma(\tau) < x < L(\tau), \quad (4)$$

where θ_m is the temperature in the mushy zone; $\lambda(\rho) = \lambda_s(1-p) + \lambda_l p$; C_l and C_s are the heat capacities in the liquid and solid phases, respectively; ρ_l and ρ_s are the liquid and solid phase densities, respectively; and λ_l and λ_s are the liquid and solid phase thermal conductivities, respectively.

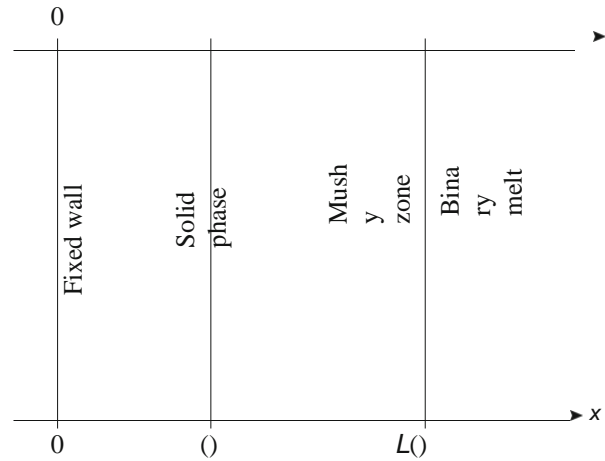


Fig. 1. Schematic diagram for the directional solidification with a mushy zone.

Heat conduction equations in the solidified material ($0 < x < \Sigma(\tau)$) and the melt ($x > L(\tau)$) are written in the form

$$\frac{\partial \theta_s}{\partial \tau} = a_s \frac{\partial^2 \theta_s}{\partial x^2}, \quad 0 < x < \Sigma(\tau), \quad (5)$$

$$\frac{\partial \theta}{\partial \tau} = a_l \frac{\partial^2 \theta}{\partial x^2}, \quad x > L(\tau), \quad (6)$$

where θ_s and θ_l are the solid and molten phase temperatures, respectively, and a_s and a_l are the thermal diffusivities of these phases, respectively.

As a boundary condition on the solid surface $x = 0$, we use a fixed temperature, i.e.,

$$\theta_s = \theta_0, \quad x = 0. \quad (7)$$

At the surface between the solid phase and the mushy zone, we have the following boundary conditions of temperature continuity and heat and mass balance:

$$\theta_s = \theta_m = \theta^* - m c_m,$$

$$(1-k) c_m \frac{d\Sigma}{d\tau} = -D_l \frac{\partial c_m}{\partial x}, \quad x = \Sigma(\tau), \quad (8)$$

$$\lambda_s \frac{\partial \theta_s}{\partial x} - \lambda(\rho) \frac{\partial \theta_m}{\partial x} = \rho L_V \frac{d\Sigma}{d\tau}, \quad x = \Sigma(\tau), \quad (9)$$

where k is the impurity distribution coefficient, L_V is the latent heat of solidification, θ^* is the phase transition temperature of the pure (without impurity) melt,

and m is the slope of the liquidus line.

$$\frac{\partial x}{\partial \tau}$$

At the mushy zone–melt boundary, the following continuity conditions of temperature, impurity concentration, and impurity fluxes, are met:

$$\begin{aligned} \theta_m &= \theta_l, \quad c_m = c_l, \quad \frac{\partial \theta_m}{\partial x} = \frac{\partial \theta_l}{\partial x}, \\ \frac{\partial c_m}{\partial x} &= \frac{\partial c_l}{\partial x}, \quad x = L(\tau). \end{aligned} \quad (10)$$

The temperature ($\theta_{l\infty}$) and the impurity concentration ($C_{l\infty}$) far from the $L(\tau)$ boundary in the liquid phase are taken to be set, i.e.,

$$\theta_l \rightarrow \theta_{l\infty}, C_l \rightarrow C_{l\infty}, x \rightarrow \infty. \quad (11)$$

We represent the volume fraction of the liquid phase in the mushy zone using the following space-time scaling dependence [40, 41]:

$$\rho(x) = \left[\frac{x}{a} + 1 - a \right]^{D-1},$$

where D is the scaling parameter and a is the parameter approximating the function $\rho(x)$. Note that the $\rho(x)$ function can be determined using the nonequilibrium mushy zone model [42–44]. However, this approach requires solving a very complex integro-differential model with moving boundaries.

SELF-SIMILAR SOLUTIONS

We search for the solution of model (2)–(12) using the following self-similar variables and dimensionless parameters:

$$\begin{aligned} \eta &= \frac{x}{D\tau}, \quad \alpha = \frac{L}{D\tau}, \quad \beta = \frac{\Sigma}{D\tau}, \\ \rho_s &= \frac{\rho_s}{\rho_{l\infty}}, \quad \rho_l = \frac{\rho_l}{\rho_{l\infty}}, \quad \rho_m = \frac{\rho_m}{\rho_{l\infty}}, \\ q &= \frac{q}{C_{l\infty}}, \quad q_l = \frac{q_l}{C_{l\infty}}, \quad p = \frac{p}{C_{l\infty}}, \\ \Lambda &= \frac{\lambda_s}{\lambda}, \quad p^* = \frac{\theta^*}{mc}, \quad \rho_{l\infty} = \frac{\theta_{l\infty}}{mc}. \end{aligned} \quad (13)$$

Integrating Eqs. (2)–(6) in variables (13) and rewriting conditions (7)–(11) using them, we obtain

$$q_m(\eta) = C_1 + C_2 \int_{\beta}^{\eta} \frac{\eta \exp(-y^2/4)}{\rho(y)} dy, \quad \beta < \eta < \alpha, \quad (14)$$

$$\rho_m(\eta) = C_5 + C_6 \int_{\beta}^{\eta} \frac{J(y) dy}{g(y)}, \quad \beta < \eta < \alpha, \quad (15)$$

$$q_l(\eta) = C_3 + C_4 \int_{\alpha}^{\eta} \exp(-y^2/4) dy, \quad \eta > \alpha, \quad (16)$$

$$\rho_s(\eta) = \rho_0 + C_7 \int_0^{\eta} \exp\left(-\frac{\varepsilon_s y^2}{4}\right) dy, \quad 0 < \eta < \beta, \quad (17)$$

$$\rho_l(\eta) = C_8 + C_9 \int_{\alpha}^{\eta} \exp\left(-\frac{\varepsilon_l y^2}{4}\right) dy, \quad \eta > \alpha. \quad (18)$$

Here, we introduced the following designations: $\varepsilon_s =$

$$D/a_s, \quad \varepsilon_l = D/a_l,$$

$$\rho(y) = \left[\frac{ay + 1 - a}{\alpha} \right]^{D-1}, \quad g(y) = \rho(y) + \Lambda(1 - \rho(y)),$$

$$J(y) = \exp\left[-\frac{D}{\alpha} \int_0^y \frac{(\rho(y) + \Lambda a_l a_s)^{-1} (1 - \rho(y)) y dy}{g(y)} \right].$$

Arbitrary constants C_i ($i = 1 \dots 9$) and parameter β (12) are specified by the following boundary conditions:

$$\frac{1 - k}{2} \beta q_m = -\frac{dq_m}{d\eta}, \quad \eta = \beta, \quad (19)$$

$$\begin{aligned} \Lambda \frac{d\rho_s}{d\eta} - \rho + \Lambda(1 - \rho) \frac{d\rho_m}{d\eta} &= G\rho\beta, \\ G &= \frac{d\eta}{2\lambda_l mc_{l\infty}}, \quad \eta = \beta, \end{aligned} \quad (20)$$

$$\begin{aligned} \rho_m &= \rho_l, \quad q_m = q_l, \\ \frac{d\rho_m}{d\eta} &= \frac{d\rho_l}{d\eta}, \quad \frac{dq_m}{d\eta} = \frac{dq_l}{d\eta}, \quad \eta = \alpha, \end{aligned} \quad (21)$$

$$\rho_l \rightarrow \rho_{l\infty}, \quad q_l \rightarrow 1, \quad \eta \rightarrow \infty. \quad (22)$$

Thus, the impurity concentration and temperature distribution in the two-phase system are determined by solutions (14)–(18), and nine arbitrary constants and parameter β (which characterizes the solid-mushy zone boundary velocity) are specified by ten

boundary conditions (19)–(22).

CONCLUSIONS

The obtained analytical solution is shown in

Figs. 2–4 for Al–Cu and Fe–Ni alloys. Figures 2a–4a show that the interface velocity (solidification rate

$d\Sigma/d\tau = \beta(2D/\tau)$) increases with scaling parameter D .

Figures 2b–4b illustrate that the volume fraction of

the liquid phase at the phase transition boundary $x = \Sigma$ decreases with increasing scaling coefficient. This means that, as D increases, the free space between growing solid structures decreases. A decrease in dimensionless temperature p_0 of the cooled boundary leads to an increase in the solidification rate (Figs. 2a, 3a) and the fraction of the liquid phase ρ (Figs. 2b, 3b). Figure 4 shows the effect of changing parameter a (which determines the solidified substance density in the phase transformation region) on the solidification rate and the bound-

ary fraction of the liquid. When this parameter increases, the velocity $d\Sigma/d\tau$ increases and the fraction of the liquid phase ρ decreases at a fixed value of scaling parameter D .

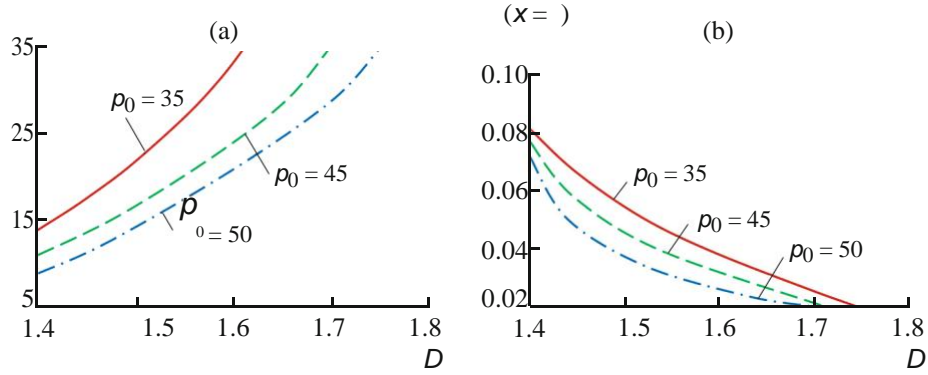


Fig. 2. Parabolic growth constant β and the fraction of liquid phase ρ at the solid-mushy zone boundary (at $x = \Sigma$ or $\eta = \beta$) vs. D .

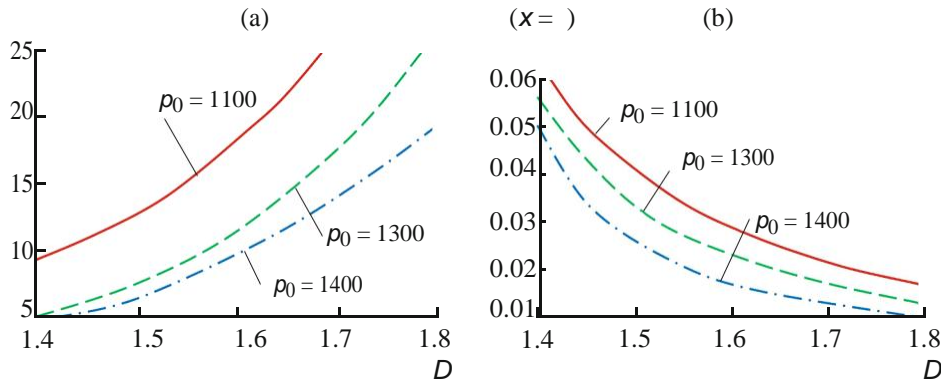


Fig. 3. Parabolic growth constant β and the fraction of liquid phase ρ at the solid-mushy zone boundary (at $x = \Sigma$ or $\eta = \beta$) vs. scaling parameter D for an Fe-0.38 wt % Ni alloy: $k = 0.68$, $\Lambda = 1.76$, $a = 1$, $G = 0.2$, $p^* = 1529.5$, $\epsilon_I = \epsilon_S = 10^{-4}$, $\alpha = 7071$, and $\rho_{I\infty} = 1700$.

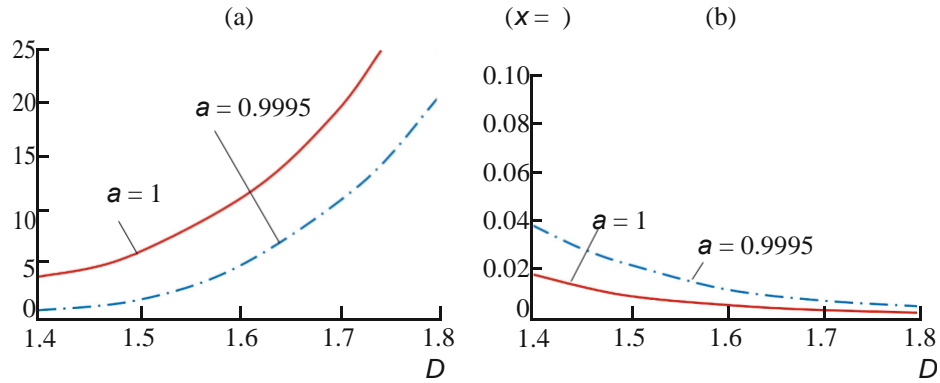


Fig. 4. Parabolic growth constant β and the fraction of liquid phase ρ at the solid-mushy zone boundary (at $x = \Sigma$ or $\eta = \beta$) vs. scaling parameter D for an Al-0.4 wt % Cu alloy: $k = 0.17$, $\Lambda = 2.32$, $\rho_0 = 500$, $G = 0.1$, $p^* = 660$, $\epsilon_I = \epsilon_S = 10^{-4}$, $\alpha = 7071$, and $\rho_{I\infty} = 800$.

The scaling theory of the mushy zone, which is developed in this work and describes the solidification of two-component melts, can be generalized to the solidification of three-component systems with main and cotectic two-phase regions using experimental data and the theory from [45–50].

FUNDING

This work was supported by the Russian Foundation for Basic Research (project no. 18-58-00034 Bel_a) and the Belarussian Foundation for Basic Research (project no. F18R-195).

REFERENCES

1. B. Ya. Lyubov, *Theory of Solidification in Large Volume* (Nauka, Moscow, 1975).
2. N. A. Avdonin, *Mathematical Description of Solidification Processes* (Zinatne, Riga, 1980).
3. Yu. A. Buvevich, D. V. Alexandrov, and V. V. Mansurov, *Macrokinetics of Crystallization* (Begell House, New York, 2001).
4. D. V. Alexandrov and P. K. Galenko, “Boundary integral approach for propagating interfaces in a binary non-isothermal mixture,” *Physica A* **469**, 420–428 (2017).
5. P. K. Galenko, D. V. Alexandrov, and E. A. Titova, “The boundary integral theory for slow and rapid curved solid/liquid interfaces propagating into binary systems,” *Phil. Trans. R. Soc. A* **378**, 20170218 (2018).
6. W. Kurz and D. J. Fisher, *Fundamentals of Solidification* (Trans. Tech. Publ., Aedermannsdorf, 1989).
7. P. K. Galenko, “Rapid advancing of the solid-liquid interface in undercooled alloys,” *Mater. Sci. Eng. A* **375–377**, 493–497 (2004).
8. P. K. Galenko, D. A. Danilov, and D. V. Alexandrov, “Solute redistribution around crystal shapes growing under hyperbolic mass transport,” *Int. J. Heat Mass Transfer* **89**, 1054–1060 (2015).
9. D. V. Alexandrov and P. K. Galenko, “Selected mode for rapidly growing needle-like dendrite controlled by heat and mass transport,” *Acta Mater.* **137**, 64–70 (2017).
10. G. P. Ivantsov, “‘Diffusion’ supercooling during solidification of a binary alloy,” *Dokl. Akad. Nauk SSSR* **LXXXI**, 179–182 (1951).
11. M. G. Worster, “Solidification of an alloy from a cooled boundary,” *J. Fluid. Mech.* **167**, 481–501 (1986).
12. D. V. Alexandrov, A. G. Churbanov, and P. N. Vabishchevich, “Emergence of a mushy region in processes of binary melt solidification,” *Int. J. Fluid Mech. Res.* **26**, 248–264 (1999).
13. D. V. Alexandrov, “On the theory of the formation of the two-phase concentration-supercooling region,” *Dokl. Phys.* **48**, 481–486 (2003).
14. W. W. Mullins and R. F. Sekerka, “Stability of a planar interface during solidification of a dilute binary alloy,” *J. Appl. Phys.* **35**, 444–451 (1964).
15. R. F. Sekerka, “Morphological stability,” *J. Cryst. Growth* **3–4**, 71–81 (1968).
16. R. T. Delves, “The theory of the stability of the solid-liquid interface under constitutional supercooling (II),” *Phys. Stat. Sol.* **17**, 119–130 (1966).
17. D. V. Alexandrov and A. O. Ivanov, “Dynamic stability analysis of the solidification of binary melts in the presence of a mushy region: changeover of instability,” *J. Cryst. Growth* **210**, 797–810 (2000).
18. D. V. Alexandrov, “Self-similar solidification: morphological stability of the regime,” *Int. J. Heat Mass Transfer* **47**, 1383–1389 (2004).
19. D. V. Alexandrov and A. P. Malygin, “Convective instability of directional solidification in a forced flow: the role of brine channels in a mushy layer on nonlinear dynamics of binary systems,” *Int. J. Heat Mass Transfer* **54**, 1144–1149 (2011).
20. D. V. Alexandrov and A. P. Malygin, “Transient nucleation kinetics of crystal growth at the intermediate stage of bulk phase transitions,” *J. Phys. A: Math. Theor.* **46**, 455101 (2013).
21. D. V. Alexandrov, “Nucleation and crystal growth in binary systems,” *J. Phys. A: Math. Theor.* **47**, 125102 (2014).
22. D. V. Alexandrov and I. G. Nizovtseva, “Nucleation and particle growth with fluctuating rates at the intermediate stage of phase transitions in metastable systems,” *Proc. R. Soc. A* **470**, 20130647 (2014).
23. D. V. Alexandrov, “On the theory of transient nucleation at the intermediate stage of phase transitions,” *Phys. Lett. A* **378**, 1501–1504 (2014).
24. V. T. Borisov, *Theory of the Two-Phase Zone of a Metal Ingot* (Metallurgiya, Moscow, 1987).
25. M. Flemings, *Solidification Processing* (McGraw Hill, New York, 1974).
26. B. Chalmers, *Principles of Solidification* (Wiley, New York, 1964).
27. D. Herlach, P. Galenko, and D. Holland-Moritz, *Metastable Solids from Undercooled Melts* (Elsevier, Amsterdam, 2007).
28. R. N. Hills, D. E. Loper, and P. H. Roberts, “A thermodynamically consistent model of a mushy zone,” *Q. J. Appl. Math.* **36**, 505–539 (1983).
29. A. C. Fowler, “The formation of freckles in binary alloys,” *IMA J. Appl. Math.* **35**, 159–174 (1985).
30. D. V. Alexandrov, A. P. Malygin, and I. V. Alexandrova, “Solidification of leads: approximate solutions of nonlinear problem,” *Ann. Glaciol.* **44**, 118–122 (2006).
31. S. Martin and P. Kauffman, “The evolution of under-ice melt ponds, or double diffusion at the freezing point,” *J. Fluid Mech.* **64**, 507–527 (1974).
32. M. G. Worster, “Convection in mushy layers,” *Annu. Rev. Fluid Mech.* **29**, 91–122 (1997).
33. T. P. Schulze and M. G. Worster, “A time-dependent formulation of the mushy-zone free-boundary problem,” *J. Fluid Mech.* **541**, 193–202 (2005).
34. D. V. Alexandrov and A. P. Malygin, “Self-similar solidification of an alloy from a cooled boundary,” *Int. J. Heat Mass Transfer* **49**, 763–769 (2006).
35. R. C. Kerr, A. W. Woods, M. G. Worster, and H. E. Huppert, “Solidification of an alloy cooled from

- above. Part I. Equilibrium growth,” J. Fluid Mech. **216**, 323–342 (1990).
36. D. V. Alexandrov and A. P. Malygin, “Coupled convective and morphological instability of the inner core boundary of the Earth,” Phys. Earth Planet. Inter. **189**, 134–141 (2011).
 37. D. W. R. Jones and M. G. Worster, “Fluxes through steady chimneys in a mushy layer during binary alloy solidification,” J. Fluid Mech. **714**, 127–151 (2013).
 38. D. V. Alexandrov, I. A. Bashkirtseva, and L. B. Ryashko, “Nonlinear dynamics of mushy layers induced by external stochastic fluctuations,” Phil. Trans. R. Soc. A **376**, 20170216 (2018).
 39. D. V. Alexandrov, A. A. Ivanov, and I. V. Alexandrova, “Analytical solutions of mushy layer equations describing directional solidification in the presence of nucleation,” Phil. Trans. R. Soc. A **376**, 20170217 (2018).
 40. D. V. Alexandrov and A. O. Ivanov, “Scaling properties of a two-phase zone in directional solidification,” Dokl. Phys. **47**, 499–503 (2002).
 41. T. Vicsek, *Fractal Growth Phenomena* (World Scientific, Singapore, 1989).
 42. V. V. Mansurov, “The nonlinear dynamics of solidification of a binary melt with a nonequilibrium mushy region,” Math. Comput. Modell. **14**, 819–821 (1990).
 43. D. L. Aseev and D. V. Alexandrov, “Directional solidification of binary melts with a nonequilibrium mushy layer,” Int. J. Heat Mass Transfer **49**, 4903–4909 (2006).
 44. D. L. Aseev and D. V. Alexandrov, “Nonlinear dynamics for the solidification of binary melt with a nonequilibrium two-phase zone,” Phys. Dokl. **51**, 291–295 (2006).
 45. A. Aitta, H. E. Huppert, and M. G. Worster, “Diffusion-controlled solidification of a ternary melt from a cooled boundary,” J. Fluid Mech. **432**, 201–217 (2001).
 46. D. M. Anderson, “A model for diffusion-controlled solidification of ternary alloys in mushy layers,” J. Fluid Mech. **483**, 165–197 (2003).
 47. D. V. Alexandrov and A. A. Ivanov, “The Stefan problem of solidification of ternary systems in the presence of moving phase transition regions,” J. Exper. Theor. Physics. **108**, 821–829 (2009).
 48. D. V. Alexandrov and A. A. Ivanov, “Solidification of a ternary melt from a cooled boundary, or nonlinear dynamics of mushy layers,” Int. J. Heat Mass Transfer **52**, 4807–4811 (2009).
 49. D. V. Alexandrov, “Nonlinear dynamics of solidification in three-component systems,” Dokl. Phys. **53**, 471–475 (2008).
 50. D. V. Alexandrov and A. A. Ivanov, “Nonlinear dynamics of directional solidification of ternary solutions with mushy layers,” Heat Mass Transfer **45**, 1467–1472 (2009).